





# Role of endothelium-pericyte signaling in capillary blood flow response to neuronal activity

Journal of Cerebral Blood Flow & Metabolism  
2021, Vol. 41(8) 1873–1885  
© The Author(s) 2021  
Article reuse guidelines:  
sagepub.com/journals-permissions  
DOI: 10.1177/0271678X211007957  
journals.sagepub.com/home/jcbfm



Wenri Zhang<sup>1,\*</sup>, Catherine M Davis<sup>1,\*</sup> ,  
Douglas M Zeppenfeld<sup>1</sup> , Kirsti Golgotiu<sup>1</sup>, Marie X Wang<sup>2,3</sup> ,  
Mariya Haveliwala<sup>2,3</sup>, Daniel Hong<sup>1</sup>, Yuandong Li<sup>4</sup>,  
Ruikang K Wang<sup>4</sup>, Jeffrey J Iliff<sup>1,2,3</sup> and Nabil J Alkayed<sup>1,5</sup> 

## Abstract

Local blood flow in the brain is tightly coupled to metabolic demands, a phenomenon termed functional hyperemia. Both capillaries and arterioles contribute to the hyperemic response to neuronal activity via different mechanisms and timescales. The nature and specific signaling involved in the hyperemic response of capillaries versus arterioles, and their temporal relationship are not fully defined. We determined the time-dependent changes in capillary flux and diameter versus arteriolar velocity and flow following whisker stimulation using optical microangiography (OMAG) and two-photon microscopy. We further characterized depth-resolved responses of individual capillaries versus capillary networks. We hypothesized that capillaries respond first to neuronal activation, and that they exhibit a coordinated response mediated via endothelial-derived epoxyeicosatrienoates (EETs) acting on pericytes. To visualize peri-capillary pericytes, we used Tie2-GFP/NG2-DsRed mice, and to determine the role of endothelial-derived EETs, we compared cerebrovascular responses to whisker stimulation between wild-type mice and mice with lower endothelial EETs (Tie2-hsEH). We found that capillaries respond immediately to neuronal activation in an orchestrated network-level manner, a response attenuated in Tie2-hsEH and inhibited by blocking EETs action on pericytes. These results demonstrate that capillaries are first responders during functional hyperemia, and that they exhibit a network-level response mediated via endothelial-derived EETs' action on peri-capillary pericytes.

## Keywords

Capillaries, epoxyeicosatrienoic acid, functional hyperemia, in vivo microscopy, pericytes

Received 4 March 2021; Revised 4 March 2021; Accepted 5 March 2021

## Introduction

Neuronal activity in the brain induces local increases in blood flow, a process termed functional hyperemia. Historically, it was doubted whether capillaries play an active role in this process; capillary function was regarded as a mere interface for exchange between blood and parenchyma. In recent years, elegant studies have shown that capillaries are in fact involved in the generation of functional hyperemia.<sup>1,2</sup>

While participation of capillaries in control of brain blood flow and functional hyperemia is now accepted,<sup>3,4</sup> details regarding the precise temporal and signaling mechanisms contributing to this phenomenon remain contradictory. Specifically, there is

<sup>1</sup>Department of Anesthesiology & Perioperative Medicine, Oregon Health & Science University, Portland, OR, USA

<sup>2</sup>Mental Illness Research, Education and Clinical Center, VA Puget Sound Health Care Center, Seattle, WA, USA

<sup>3</sup>Department of Psychiatry and Behavioral Sciences, University of Washington School of Medicine, Seattle, WA, USA

<sup>4</sup>Department of Bioengineering, University of Washington School of Medicine, Seattle, WA, USA

<sup>5</sup>Knight Cardiovascular Institute, Oregon Health & Science University, Portland, OR, USA

\*The first two authors contributed equally to this work.

### Corresponding author:

Nabil J Alkayed, Department of Anesthesiology & Perioperative Medicine and Knight Cardiovascular Institute, Oregon Health & Science University, 3181 SW Sam Jackson Park Road, Portland, OR 97239, USA.  
Email: alkayedn@ohsu.edu

disagreement regarding the timing of the responses of different order vessels to neuronal activation, with some studies demonstrating that the arteriolar response precedes the capillary response, and vice versa.<sup>1,2,5</sup> Furthermore, whereas arteriolar dilation serves to increase blood flow in response to increased energy demand, it is not clear what function the capillary response serves, how different it is from that of arterioles, and how the two are coordinated.

Capillaries were traditionally thought of as passive players in the hyperemic response due to their lack of contractile vascular smooth muscle cells (VSMCs). However more recent studies, both in cerebral cortex and retina, have shown that pericytes are contractile cells that are can regulate capillary blood flow.<sup>1,3,5–8</sup> Pericytes are part of the neurovascular unit (NVU), lodged between capillary endothelium and astrocytic end feet. Brain capillaries have a much higher coverage of pericytes than peripheral capillaries, highlighting their importance to cerebrovascular regulation. Pericytes are analogous to VSMCs in that they express contractile proteins such as alpha-smooth muscle actin.<sup>9</sup> However, the concept that pericytes control brain capillary blood flow, basally or during functional hyperemia, remains controversial; some studies suggest that pericytes mediate functional hyperemia, others show that while pericytes are contractile they do not mediate physiological functional hyperemia, and yet others suggest that pericytes are not contractile and that functional hyperemia is solely regulated by arteriolar smooth muscle cells, not by capillary pericytes.<sup>1,10,11</sup>

Finally, the identity of the specific cell-cell signaling involved in regulating capillary blood flow has not been fully elucidated.<sup>4</sup> We previously demonstrated a role for astrocyte-derived metabolites of arachidonic acid called epoxyeicosatrienoates (EETs) in arteriolar dilation following neuronal activation.<sup>12–15</sup> In light of new knowledge implicating capillaries in functional hyperemia, we investigated the role of EETs in coupling neuronal activity to capillary blood flow response.

In this study, we characterize the capillary response to the generation of functional hyperemia in the murine whisker barrel cortex, and further define the source and role of EETs. We asked first whether capillaries are involved in the hyperemic response to whisker stimulation, and if so, how is the capillary response temporally related to that of arterioles. Furthermore, we compared responses of individual capillaries versus capillary networks, and responses of capillaries at different cortical layers. We used *in vivo* two-photon microscopy (2-PM) to directly visualize cortical capillaries of the mouse whisker barrel cortex through an open skull window preparation before, during, and after whisker

stimulation. To visualize pericytes and cerebral vessels, we either used wild-type (WT) mice injected with FITC- conjugated dextran, or Tie2-GFP/NG2-DsRed mice, which have endothelial cells and pericytes fluorescently labeled in green and red, respectively. Additionally, we used optical microangiography (OMAG) as previously described<sup>16,17</sup> to measure capillary flux, a parameter assessing the number of RBCs passing per unit time that is directly related to oxygen delivery. We found that capillaries respond ahead of arterioles, and in contrast to arterioles, they exhibit a coordinated response that serves to redistribute blood flow within the capillary network. Finally, the response involves endothelial-pericyte crosstalk in part mediated via the action of endothelia-derived EETs on pericytes.

## Materials and methods

### Animals

This study was conducted in accordance with the National Institutes of Health guidelines for the care and use of animals in research, and protocols were approved by the Institutional Animal Care and Use Committee at Oregon Health and Science University, Portland, OR, USA. Reporting of results conforms to ARRIVE 2.0 (Animal Research: Reporting on In Vivo Experiments) guidelines.<sup>18</sup> Adult male mice (3–4 months old, 25–30 g) were used. Wild-type C57BL/6J, Tg(TIE2GFP)287Sato/J and Tg(Cspg4-DsRed.t1)1Akik/J mice were purchased from the Jackson Laboratory. To generate mice with endothelial cells and pericytes fluorescently labeled in green (GFP) and red (DsRed), respectively, Tg(TIE2GFP)287Sato/J mice were bred with Tg(Cspg4-DsRed.t1)1Akik/J; the progeny termed Tie2-GFP/NG2-DsRed. Mice with endothelial-specific over-expression of sEH (Tie2-hsEH) were also used, as previously described.<sup>19</sup>

### Open skull window preparation

Twenty-four hours prior to experiment, cranial window surgery was performed, please see *Supplemental Methods* for details.

### Air puff whisker stimulation

Please see *Supplemental Methods* for details of equipment and animal preparation.

### Whisker stimulus parameters

Mice were exposed to 15 psi air puff whisker stimulus of 5 Hz for 10 s (stimulus) or no air puff (control). Whisker stimulus duration was 10 s, preceded by 30 s of baseline recording (no stimulus), followed by 45 s of

post-stimulus recording. Between the end of a post-stimulus session and the beginning of the baseline session of the next stimulus event, a 5-min wait time occurred to allow vasculature normalization and recovery between stimulus events. Air puff was delivered as an air sheet with a pressure of 15 psi, at 5 Hz/s, with no delay in between puffs.

### *Micropipette puff stimulation*

For micropipette puffing experiments using Tie2-GFP/NG2-DsRed mice, a craniotomy was performed in place of the thin skull and the dura carefully removed. The brain was protected with 1% agar and a coverslip was placed over 60% of the window to allow a glass pipette to access the cortex. A 3- $\mu$ m tip diameter glass pipette pulled with a long taper was filled with one of three solutions: (1) 14,15-epoxyeicosa-5(Z)-enoic acid (14–15 EEZE; 100  $\mu$ M; Cayman Chemical) in 0.1% DMSO in artificial cerebrospinal fluid (aCSF; 125 mM NaCl, 26.2 mM NaHCO<sub>3</sub>, 2.5 mM KCl, 1.25 mM NaH<sub>2</sub>PO<sub>4</sub>, 1.0 mM MgCl<sub>2</sub>, 2 mM CaCl<sub>2</sub>, 25 mM glucose); (2) 100  $\mu$ M ATP (Sigma) in aCSF; or (3) vehicle (0.1% DMSO in aCSF). The concentration of 14,15-EEZE was calculated to be 10 times the effective concentration at the tissue target, with the expectation that drug concentration will drop to its effective concentration as it diffuses to the tissue target. In previous studies conducted *in vitro*, we and others have used EEZE at 10  $\mu$ M.<sup>20,21</sup> Texas Red Dextran (10-kD; Sigma) was also added to visualize the pipette with 2-PM. The glass pipette was carefully lowered at least 100  $\mu$ m into the cortex at a 14° angle without puncturing any major vessels with an MMP225 micromanipulator (Sutter). A 70-ms, 30-psi air puff was delivered to the pipette with a picospritzer III (Harvard Apparatus), which ejected a small volume of drug to the cortex. A 40- $\mu$ m 512  $\times$  512 frame *z*-stack with 2- $\mu$ m *z*-steps was continuously acquired at 0.2- $\mu$ m/pixel before and after puff.

### *Two-photon image acquisition*

All *in vivo* imaging was carried out with a Chameleon laser (Coherent) attached to a Zeiss LSM 7MP scan head. A 20 $\times$  0.9 NA water immersion lens was used to image through the thinned skull window. An excitation wavelength of 800, 840 or 980 nm was used depending on the fluorophore. Laser power was controlled such that average power measured at the sample never exceeded 40 mW.

**Red blood cell (RBC) flux imaging – capillaries.** Three suitable regions of interest within the cranial window viewing area were selected per mouse based on clarity

criteria and density of capillaries at a depth of 100–200  $\mu$ m below the pial surface. Capillaries were identified according to the branching order classification by Cai et al.,<sup>22</sup> with some modifications; we included microvessels with branching orders 1, 2 and 3 that were of similar diameter to RBCs (<5  $\mu$ m) located within 150–200  $\mu$ m below brain surface. RBC flux was quantified using high-speed linescans perpendicular to capillaries. Continuous line scan imaging captures RBCs moving single-file through a capillary as transient absences of the FITC-dextran fluorescent signal. The total count of RBCs was normalized to total scan time to determine flux in units of RBCs/second.

**Red blood cell velocity imaging – Arterioles.** Within the above-mentioned three regions, arterioles were also selected for measurement of RBC velocity. This parameter was selected as a proxy to RBC flux as the speed and numbers of RBCs passing through larger diameter arterioles is too great; thus velocity measurements are more suitable for this vessel type. Arterioles were selected, then confirmed as arterioles by positions, vessel wall morphology, and identification of a pulse (heartbeat) bulge in a preliminary perpendicular line scan acquired prior to the parallel line scan required for velocity measurements. Line scans were taken on each individual vessel in separate treatment events with a baseline, designated treatment, and post-stimulus scan of 30, 10, and 45 s, respectively. The line to measure velocity was drawn in the midline of the vessel (parallel to vessel walls), and fluorescence intensity in these images was used as a close approximation of volumetric flow. Because FITC-dextran labels plasma in bright green, RBCs remain unlabeled and appear dark. The more RBCs passing by the line scan create a lower (darker) mean intensity value for the field of view of the scanned segment. Higher mean intensity values (brighter) would reflect fewer RBCs and more plasma (green fluorescence) passing across the line scan. Therefore, fluorescence intensity is inversely related to the number of RBCs passing across the line scan.

### *Optical microangiography*

OMAG was performed as previously described.<sup>16,17</sup> This optical coherence tomography (OCT) based angiography technique was used to visualize and quantify blood flow at the capillary level based on intrinsic light scattering properties of moving blood cells within biologic tissue, with no need to use exogenous contrasting agents.<sup>23–25</sup> A custom-built spectral domain OCT system was used, please refer to *Supplemental Methods* for a detailed description of the OMAG system. The flux and vessel diameter analyses were

targeted at a smaller volume on a 368  $\mu\text{m}$  thick swath of tissue, yielding a physical volume with the  $x$ - $y$ - $z$  dimensions:  $0.5 \times 0.5 \times 0.08$  mm, and divided into four layers that are approximately 92  $\mu\text{m}$  thick each. En-face projection of each layer was made to determine the average flux of the volume. To calculate diameter change, we used a validated algorithm previously used to assess retinal capillary diameters from the OMAG-generated OCT angiograms.<sup>26</sup>

Please see *Supplemental Methods* for detailed description of image and data analysis.

For both imaging modalities, mortality rate was below 15%. The only data excluded was from mice that did not survive scanning. Experimenter was blinded to genotype but not vessel type or stimulus. Randomization was not carried out. Statistical analysis was performed using GraphPad Prism 8.3.1 for Windows (GraphPad Software, San Diego, CA, USA).

## Results

To assess the hyperemic response to whisker stimulation, RBC flux and diameter and arteriolar velocity and mean fluorescence intensity were measured in

barrel cortex of mice using in vivo 2-PM and OMAG. Experimental set-up is illustrated in Figure 1 (a) and Supplemental Figure S1.

Capillary response to whisker stimulation precedes the arteriolar response. We first asked which vascular segment responds first to neuronal activation elicited by whisker stimulation. Capillary (flux) and arteriolar (velocity) responses to 10-s whisker stimulation (15 psi at 5 Hz/s) were evaluated by 2-PM in wild-type (WT; C57Black6/J) mice injected with 200 kD FITC-dextran to visualize vasculature. Comparison of response time between capillaries and arterioles in the barrel cortex (Figure 1,  $n = 5$ –12 vessels) show a delayed response in the arterioles. Figure 1(b) shows an overlay of mean RBC flux (dashed line) and RBC velocity (solid line) in capillaries vs. arterioles, respectively, demonstrating that the capillary response precedes, and reaches its peak prior to the arteriolar response. When quantified (Figure 1(c)), the time to 50% of peak response following whisker stimulation is significantly shorter for capillaries than arterioles,  $4.55 \pm 2.19$  s for capillaries compared to  $16.72 \pm 5.74$  for arterioles ( $P < 0.0001$ , t-test). In Supplemental Figure S2, we overlaid capillary flux (red line) with arteriolar velocity (blue line) and

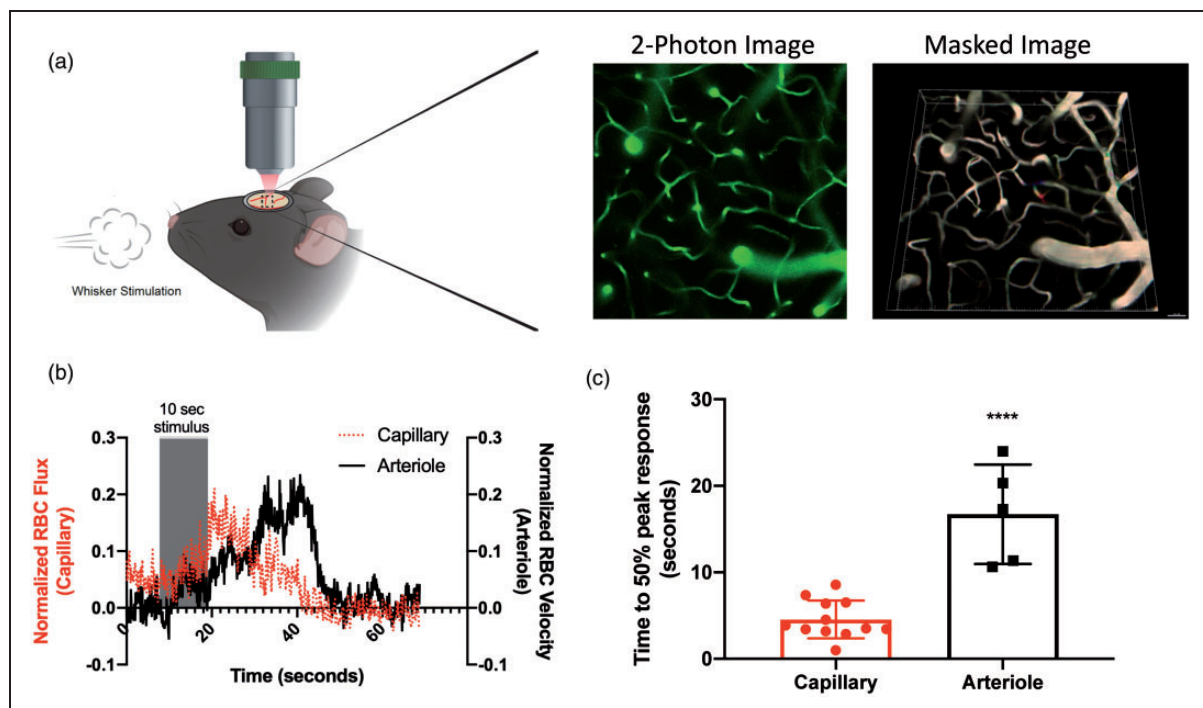


**Figure 1.** Capillary response to whisker stimulus precedes arteriolar response. Capillary and arteriolar responses to whisker stimulation were evaluated using in-vivo two-photon microscopy in WT mice injected with 200 kD FITC-dextran to visualize vasculature: (a) schematic of in-vivo experimental set-up with representative two-photon and subsequent masked images; (b) red blood cell flux (capillaries) and red blood cell velocity (arterioles) in response to 10-s whisker stimulus. Magnitude change was calculated from the pre-stimulus baseline average, and data aligned by the 10-s stimulus timeframe; (c) time to 50% peak response following whisker stimulation is shorter in capillaries than arterioles (unpaired t-test, \*\*\*\* $P < 0.0001$ ). Data represent mean  $\pm$  SD ( $n = 12$  capillaries,  $n = 5$  arterioles).

inverse mean intensity for arterioles (black line; an approximation of volumetric flow). As the figure shows, the peak of the inverse mean intensity of the arterioles has an even longer time delay than the peak of the velocity.

Capillaries exhibit a network response to functional hyperemia. We next investigated the nature of this capillary hyperemic response to neuronal activation, asking whether capillary flux uniformly increased in all capillaries, or they exhibit a variable response aimed at redistributing blood flow. When we monitored capillary flux over time under control conditions (without whisker stimulation) by 2-PM, we observed that, while many capillaries exhibited minimal change in flux as expected, both decreases and increases in flux were apparent in others (Figure 2). Upon neuronal activation, mean flux was increased from  $-0.33 \pm 7.00$  in control ( $n=6$  animals; 80 capillaries) to  $2.89 \pm 8.79\%$  ( $n=9$  animals; 57 capillaries) of baseline, illustrated by a rightward shift in the frequency distribution

curve (Figure 2(a);  $P < 0.001$ , nonlinear regression with Gaussian fit). Median change in flux increased from  $-0.66$  in control to  $3.39\%$  after neuronal stimulation (Figure 2(b);  $P < 0.05$ , Mann–Whitney U test; Kolmogorov–Smirnov test of normality showed that the stimulus data do not follow a normal distribution,  $D(0.19)$ ,  $P = 0.0059$ , hence the Mann–Whitney U test was used to compare the data distributions). Despite this overall increase in flux, some capillaries exhibited a decrease in flux, while many remained unchanged upon whisker stimulation, evident in both Figure 2(a) and (b). To further illustrate the capillary flow redistribution concept, we chose a cutoff threshold of 10% change in flux in either direction to delineate capillaries that show either an increase or decrease or no change in flux. Figure 2(c) shows that in the unstimulated group, approximately a third of capillaries undergo an increase in flux, a third show a decrease and a third show no change in flux. After whisker stimulation, we observed a higher percentage of capillaries exhibiting

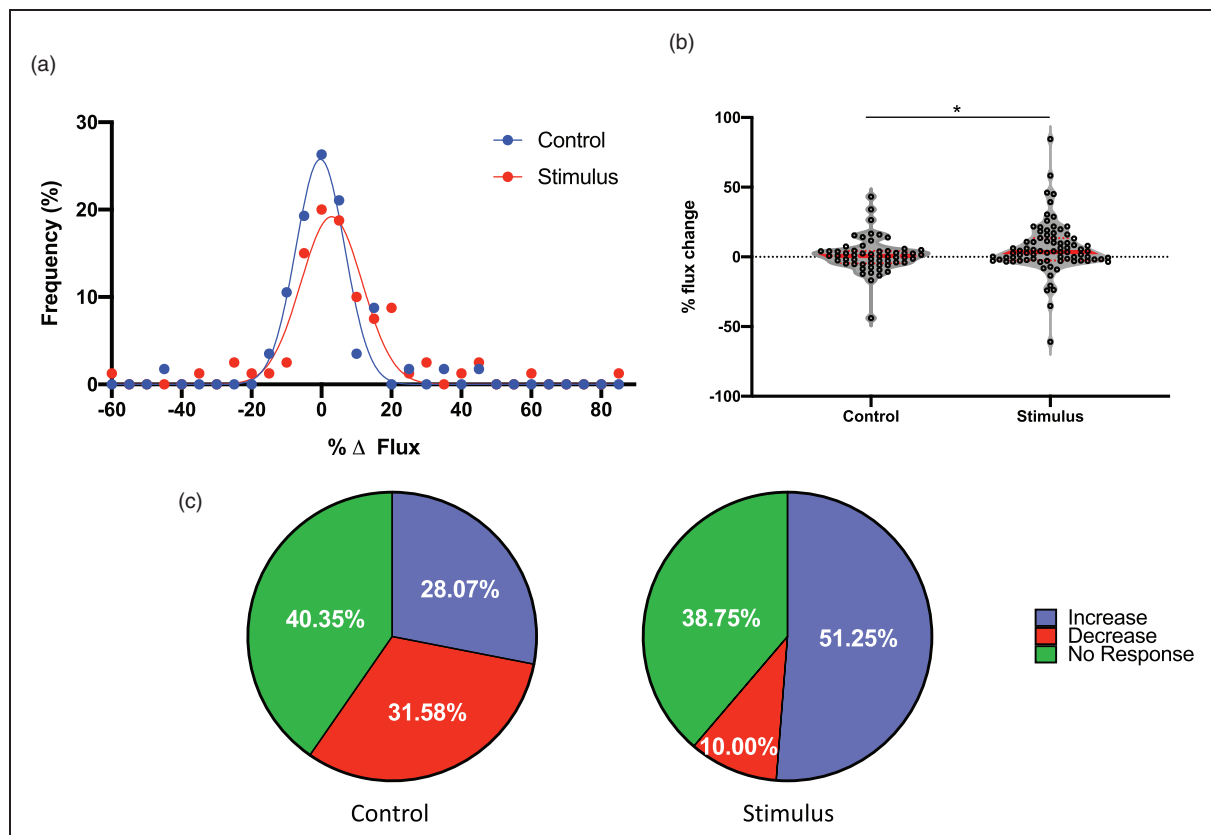


**Figure 2.** Capillaries exhibit a network response to whisker stimulation. RBC flux, used as a surrogate measurement to capillary dilation (increased flux) and constriction (decreased flux), was measured in capillaries following 10-s whisker stimulation ( $n = 57$  capillaries) as well as control (no stimulation;  $n = 80$  capillaries): (a) frequency distribution of capillary responses to whisker stimulation, or no stimulation (control;  $P < 0.001$ , nonlinear regression with Gaussian fit); (b) violin plot showing distribution of responses of every data point with median (thick red line) and interquartile ranges (thin red lines;  $*P < 0.05$ , Mann–Whitney U test); (c) pie charts depict percentage of capillaries with increased (blue), decreased (red), or no change (green) in RBC flux, where a change is classified as an increase or decrease of  $> 10\%$  of baseline.

increased flux at the expense of capillaries that exhibited a decrease in flux, with no difference in the percentage of capillaries that showed no change ( $P < 0.01$ , Chi square test). This observation suggests that the entire capillary bed responds to functional neuronal activation by redistributing capillary blood flow, likely shifting blood flow to capillaries adjacent to active neurons.

Inhibition of 14,15-EET signaling induces capillary constriction. We have previously reported that 14,15-EET signaling contributes to neurovascular coupling, signaling from astrocytes to arteriolar vascular smooth muscles.<sup>4,27</sup> The eicosanoid is also released by endothelial cells, where it has been postulated as an endothelial-derived hyperpolarizing factor (EDHF) in small caliber vessels.<sup>28</sup> Pericytes are the only contractile cells in capillaries, and have been proposed to regulate capillary flux in response to neuronal activity. Therefore, we

asked whether pericytes regulate capillary flux via 14,15-EET. To test this hypothesis, we used a micropipette attached to a picospritzer to apply EETs antagonist 14,15-EEZE (100  $\mu\text{M}$ , mixed with Texas Red<sup>29</sup>) directly to peri-capillary pericytes within cortical layer II. Pericytes were identified as red cells surrounding green capillaries in Tie2-GFP/NG2-DsRed mice by 2-PM (Supplemental Figure S3). As illustrated in Figure 3, upon 14,15-EEZE puff onto pericytes, the majority of capillaries constricted, suggesting a basal tone of EETs that facilitates an overall dilated capillary network. Figure 3(a) and (b) show the decrease in diameter in three capillaries after 14,15-EEZE puff; the red cloud in the right panel of Figure 3(a) represents the extent of EEZE reach (please see the video in supplemental material). Assessment of all capillaries affected by 14,15-EEZE (within the red cloud,  $n = 57$ ), revealed that compared to vehicle ( $n = 38$ )

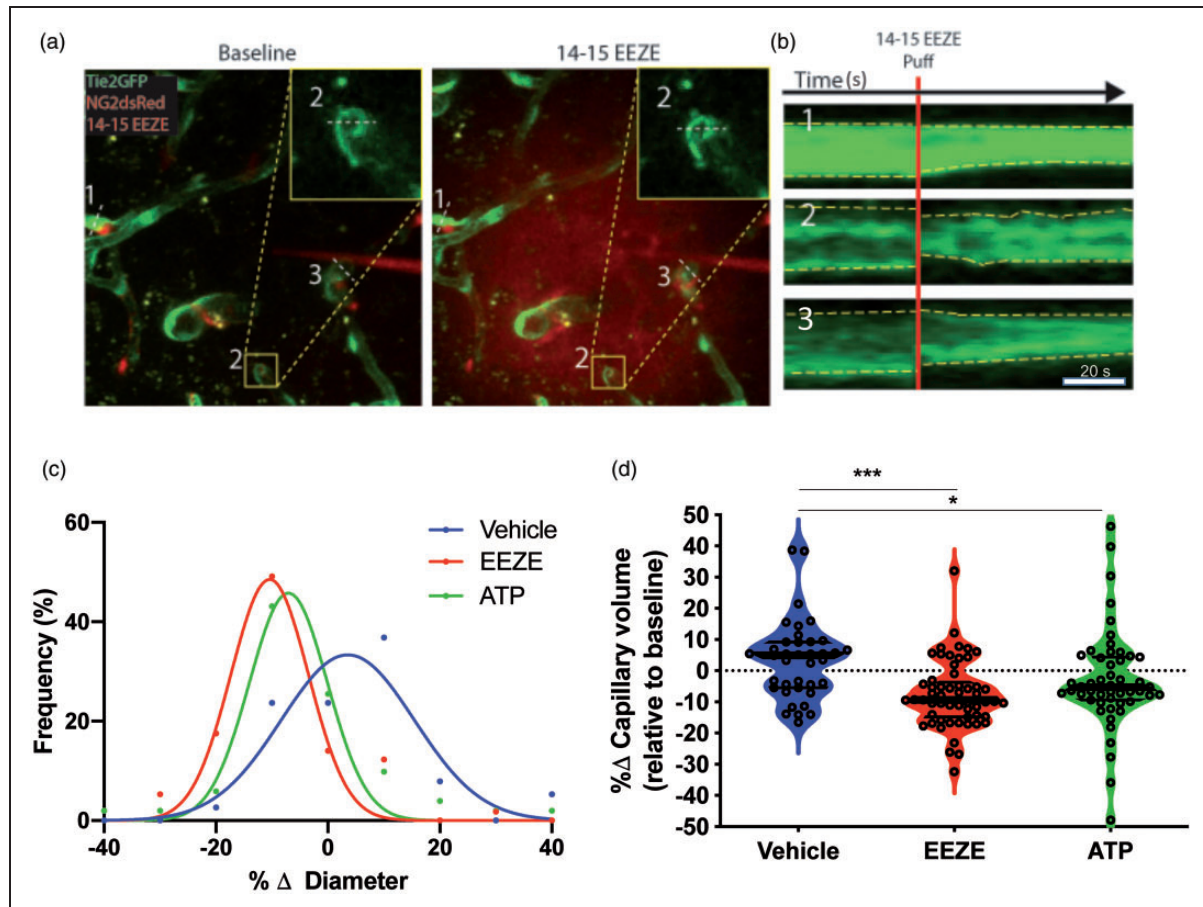


**Figure 3.** 14,15-EEZE induces capillary constriction: (a) representative z-projections within a time series before (baseline) and after puff of 100  $\mu\text{M}$  14,15-EEZE in Tie2-GFP/NG2-DsRed mice, which have endothelium fluorescently labeled green and pericytes red. Red “cloud” indicates extent of 14,15-EEZE coverage, which was mixed with 10 kD Texas Red Dextran prior to puff; (b) intensity projections over time (scale bar 20 s) of the three capillary cross sections depicted in (a); (c) frequency distribution of capillary responses for 14,15-EEZE, ATP and vehicle ( $P < 0.001$ , nonlinear regression with Gaussian fit); (d) violin plot (median, thick black line and interquartile ranges, thin black lines) of capillary responses to vehicle, 14,15-EEZE and ATP, relative to baseline (\* $P < 0.05$ , \*\*\* $P < 0.001$ , one-way ANOVA, Dunnett’s multiple comparison test;  $n = 38$  vehicle,  $n = 57$ , 14,15-EEZE,  $n = 51$  ATP).

which resulted in a  $4.24 \pm 11.51\%$  mean change in diameter, 14,15-EEZE application resulted in a constriction with  $-10.41 \pm 5.26\%$  change in diameter, illustrated by the leftward shift in the distribution curve in Figure 3(c) compared to vehicle ( $P < 0.001$ , nonlinear regression with Gaussian fit). The positive control, ATP, also resulted in a decreased mean diameter of  $-7.35 \pm 3.63\%$  ( $n = 51$ ). The net effect of these changes in diameter is a decrease in capillary volume by both 14,15-EEZE and ATP (Figure 3(d)). Interestingly, in addition to the net changes in capillary diameter and volume brought about by 14,15-EEZE and ATP, we observed that even upon application of a vasoconstricting agent, some capillaries respond by increasing capillary volume. Figure 3(d) shows the different distribution patterns between 14,15-EEZE and ATP compared to vehicle, with positive median values for vehicle and negative for 14,15-EEZE and ATP. Intriguingly, all three conditions show multimodal distributions, with peaks at approximately  $+10$  and  $-10\%$  change in capillary diameter. This observation suggests that unlike arteries and arterioles, in which vessel diameter changes over a continuum of vascular tone, capillary diameter seems to alternate between two distinct states – plus and minus the same percentage of capillary diameter ( $\sim 10\%$ ). Intra-parenchymal arterioles located within or adjacent to the volumes delineated by the fluorescent dye cloud did not respond to either EEZE or ATP, compared to vehicle, over 20 min of imaging (Supplemental Figure S4).

Endothelial over-expression of sEH abolishes capillary dilation to whisker stimulation. Since we demonstrated that blocking the action of 14,15-EET on capillary pericytes induced vessel constriction, indicating that endogenous 14,15-EET signals to pericytes to regulate capillary response, we sought to determine the source of this 14,15-EET. We investigated cerebrocortical capillary response to whisker stimulation in mice over-expressing the EET-degrading enzyme soluble epoxide hydrolase (sEH; Tie2hsEH) compared to their WT littermate controls.<sup>19</sup> Hyperemic response was assessed at four levels, each  $92 \mu\text{m}$  thick, of increasing depth within the cerebral cortex by OMAG. When averaged across all four layers, we see an increase in capillary diameter of  $4.18 \pm 2.19\%$  in response to stimulation in WT; this response is abolished in Tie2hsEH mice where vessel diameter decreases to  $-2.03 \pm 2.01\%$  of baseline ( $n = 5$ ,  $P < 0.01$ , one-way ANOVA; Figure 4(c)). Capillary diameter in unstimulated WT sham mice remained unchanged over a time course similar to that of stimulated mice under the same experimental conditions and anesthesia ( $0.004 \pm 0.006\%$  of baseline,  $n = 3$ ). Using flux as a readout, we also found that the hyperemic response is attenuated in Tie2hsEH mice compared to WT mice. At a depth of

$93\text{--}183 \mu\text{m}$ , WT mice increase flux by  $3.58 \pm 4.47\%$  in response to stimulation, while flux in Tie2hsEH mice decreases to  $-2.88 \pm 1.80\%$  of baseline ( $n = 5$ ,  $P < 0.01$ , one-way ANOVA; Figure 4(b)). As for diameter, flux is stable over time in unstimulated WT mice ( $-0.25 \pm 1.33\%$  of baseline,  $n = 3$ ). Flux data across all layers can be found in Supplement ( $n = 5$ ,  $P < 0.05$ , two-way ANOVA with Sidak's multiple comparison test; Supplemental Figure S5).

## Discussion

Capillaries have recently been identified as active participants in functional hyperemia, challenging the traditional dogma that they are merely surfaces for exchange between blood and brain tissue parenchyma. Fundamental questions about the nature of the role of capillaries remain unresolved.<sup>1,2,5</sup> By carefully studying the hyperemic response to a physiological stimulus of whisker barrel cortex stimulation, we provide additional support to the notion that capillaries play a role in neurovascular coupling during functional hyperemia, and provide new details regarding the nature of the capillary hyperemic response, its timing relative to arteriolar dynamics, relationship to other capillaries within the network and across cortical layers, and cell-cell signaling involved.

We show that the capillary hyperemic response is generated locally to the activated neurons, and that it precedes the increase in arteriolar velocity and RBC flow. We also show that the hyperemic response of capillaries is accompanied by decreases in blood flow in other capillaries within the network. Finally, we show that the capillary functional hyperemic response is attenuated in mice with lower endothelial EETs, and that EETs inhibition constricts pericytes. Taken together, we conclude that endothelial EETs contribute to the capillary functional hyperemic response to neuronal activation by relaxing pericytes, and that this action is coordinated within the capillary network, as depicted schematically in Figure 5. These findings advance our understanding of CBF regulation and interpretation of blood oxygen level-dependent functional magnetic resonance imaging (BOLD fMRI), which relies on changes in blood flow and oxygen levels to define regions of brain activity.<sup>1,2,4,5,7</sup> While BOLD is the standard technique used to generate images in fMRI studies, many aspects of the source of BOLD signal remain unexplained by current models, such as the spatial and temporal features of the underlying hemodynamic response to neuronal activity. The possibility that endothelial signaling is initiated at the capillary level, close to active neurons, which then travels retrogradely would explain the selective recruitment of specific arterial branches and the

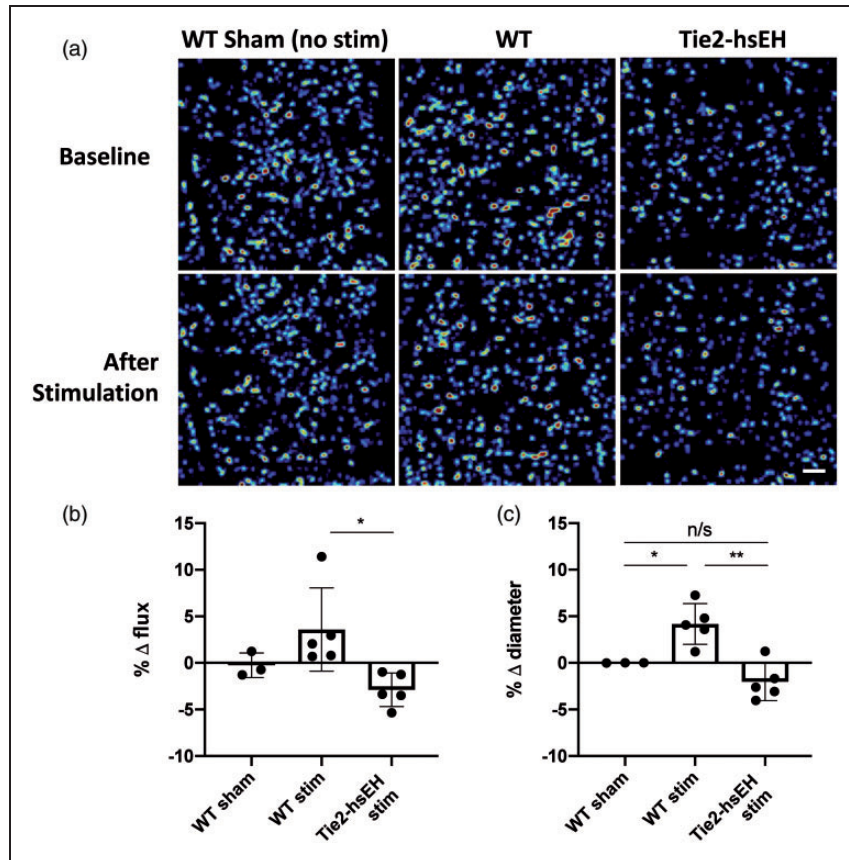


**Figure 4.** Endothelial over-expression of sEH abolishes response to whisker stimulation. Changes in capillary diameter and RBC flux were evaluated by OMAG: (a) representative OMAG flux images, acquired at 93–183  $\mu\text{m}$  cortical depth, scale bar 50  $\mu\text{m}$ ; (b) percentage change in RBC flux in cortex (93–183  $\mu\text{m}$  depth); (c) capillary diameter in cortex (1–368  $\mu\text{m}$ ) in response to whisker stimulation in Tie2hsEH (endothelial-specific over-expression of sEH) and WT control mice (\* $P < 0.05$ , \*\* $P < 0.01$ , n/s not significant, one-way ANOVA). Data represent mean  $\pm$  SD ( $n = 3\text{--}5$ ).

optimal, locally localized blood flow response. Most neurovascular coupling research has focused on the role of extravascular cells, such as astrocytes and neurons, in generating the vasoactive mediators of neurovascular coupling. Our data support a model whereby EETs are released by the capillary endothelium, removing the need for extravascular signaling at the level of arterioles. Although the dilation of arteries and arterioles can be significant, their small volume and high oxygenation means that arteries themselves contribute relatively little to the fMRI BOLD signal. Veins, on the other hand, exhibit large increases in deoxyhemoglobin that contribute significantly to the fMRI BOLD signal. However, these increases are expected to be both delayed, and to be weighted superficially and medially with respect to the active capillary beds, as a result of the venous drainage pattern.<sup>30</sup> Our findings are also relevant to the concept of capillary transit time heterogeneity (CTH), a determinant of delivery of substances from the blood to the brain tissue originally suggested by Kuchinsky and Paulson.<sup>31</sup> Recent studies have

shown that capillary blood flow heterogeneity changes during functional hyperemia, reflecting a locally coordinated capillary response to neuronal activation, a response that may be impaired in disease states.<sup>32–34</sup> Finally, “resting-state” fluctuations in resting-state fMRI (rsfMRI), used to assess functional connectivity of distant component of large-scale neural systems, likely reflects capillary fluctuations in response to basal neuronal activity.<sup>35–37</sup>

The question of the temporal onset of hyperemia in different caliber vessels lacks a consistent answer, with studies in retina and somatosensory cortex suggesting that arterioles dilate prior to capillaries in response to stimulus, and studies in the olfactory bulb showing that capillaries and arterioles have similar response times.<sup>2,5,7</sup> Our study using high-resolution, multi-modal imaging of physiological functional hyperemia in the whisker barrel cortex demonstrates that the increase in capillary flux precedes the changes in arteriolar velocity and flow, supporting a previous study in the barrel cortex.<sup>1</sup> Taken together with another study



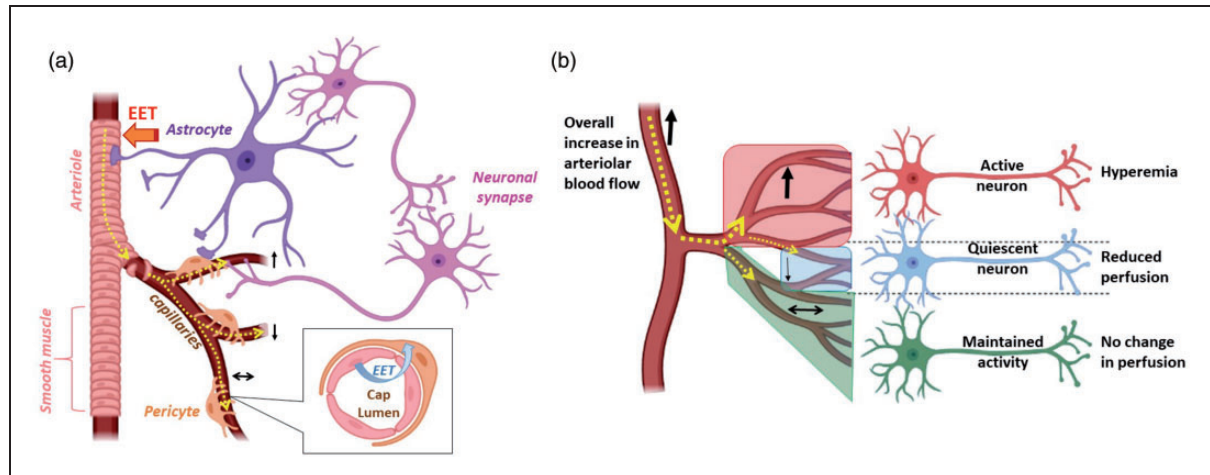


**Figure 5.** Schematic illustration of the capillary-arteriolar response to neuronal activation: (a) at baseline, capillaries alternate between dilation (upward arrow), constriction (downward arrow) and no change in diameter (left–right arrow), with an approximately similar proportion of capillaries in each state at any given time (same thickness of dotted yellow line and a single capillary representing each state); (b) upon increased neuronal activity, more capillaries dilate (hyperemia; thicker upward arrow and more capillaries within red area) than constrict (thinner downward arrow, with less number of capillaries within a smaller blue area), with a maintained fraction of capillaries that show no change in diameter (left–right arrow of same thickness as baseline within the green area). The result is an overall increase in arteriolar blood flow. The increase in capillary blood flow in response to neuronal activation is dependent on endothelial-derived EET’s action on pericytes, which is also required to maintain capillaries in a dilated state at baseline (inset in (a)). Created in BioRender.com.

in sensory cortex,<sup>38</sup> these contradictory reports regarding the temporal relationship between the capillary versus arteriolar response to neuronal activation may be related to the following reasons: (1) regional differences in the brain, with barrel cortex capillaries dilating prior to arterioles, (2) differences in the temporal resolution of imaging methods, (3) differences in the method used to elicit neuronal activity; i.e., a physiological *in vivo* stimulus such as whisker stimulation used in our study, compared to non-physiological stimuli such as electrical stimulation, either *in vivo* or in brain slices, used in other studies, and finally, (4) differences in spatial coverage of the hyperemic response; e.g., focusing on a capillary network in a cortical layer that may not be adjacent to the activated neurons (discussed further below).

Contractile pericytes, apposed to capillaries, extend processes both along and around capillaries, as demonstrated in Supplementary Figure S3.<sup>9,10</sup> The ability of pericytes to control brain capillary blood flow, either basally or during functional hyperemia, remains controversial.<sup>1,10,11</sup> Hall and colleagues suggested that the presence of pericytes underlies capillary dilation, with resting capillary diameter being larger in capillary segments in contact with pericyte somata and processes,<sup>1</sup> A more recent study further supported the role of pericytes in blood flow regulation, demonstrating diminished capillary responses to functional hyperemia in pericyte-deficient mice, with capillaries showing both reduced

RBC flux and a lag in response time compared to pericyte-intact mice. Interestingly, arteriolar response to neuronal stimulus was unaffected.<sup>39</sup> Our observation that capillaries respond prior to arterioles, implies that capillary-associated pericytes may either sense, or bring about changes in tone, faster than VSMCs found on arterioles. This would be consistent with the idea of retrograde dilation proposed in the study by Longden et al.<sup>40</sup> Specifically, in that study, authors proposed a central role for capillary endothelial cells in sensing neural activity and communicating it to upstream arterioles in the form of an electrical vasodilatory signal.

While the contribution of pericytes to capillary dilation is still somewhat disputed, the contribution of some vasoactive mediators, namely the vasodilator prostaglandin E<sub>2</sub> and nitric oxide, and the vasoconstrictor 20-HETE have been implicated in regulation of pericyte tone.<sup>1</sup> No studies have investigated the role of 14,15-EET, previously implicated in arteriolar functional hyperemia,<sup>12–15</sup> in pericyte-mediated regulation of capillary tone. Our observation that local application of 14,15-EEZE (14,15-EET antagonist) directly onto capillary pericytes induces capillary constriction indicates that endogenous 14,15-EET may relax pericytes to keep capillaries patent at baseline, and potentially contribute to increased capillary perfusion during hyperemia. This endogenous basal release of 14,15-EET likely reflects basal neuronal activity and contributes to “resting-state” fluctuations of capillary blood flow. The source of endogenous 14,15-EET is

either astrocytes<sup>13,27</sup> or endothelial cells. Endothelial cells both release EETs (a putative EDHF) and express EETs-generating enzymes, and capillary endothelium shares a basement membrane with pericytes and has been suggested to sense neuronal activity, making it an ideal candidate for both sensing the need for hyperemia as well as affecting pericyte tone.<sup>2,41-45</sup> In support of an endothelial origin of 14,15-EET, we show that mice with reduced endothelial EETs, due to endothelial overexpression of EETs-metabolizing enzyme sEH, exhibit an attenuated capillary response to whisker stimulation. Nonetheless, the role of astrocyte-derived EETs cannot be ruled out. Using a brain slice preparation, Mishra et al.<sup>46</sup> showed that electrical stimulation-evoked capillary dilation is reduced after blockade of PGE2 receptor EP<sub>4</sub>. Based on that evidence and lack of effect of EETs synthesis inhibition, authors concluded that EETs do not play a role in capillary functional hyperemia. However, inhibition of EETs synthesis does not eliminate the pool of already formed EETs, which is known to be stored in membrane phospholipids and ready to be released upon activation.<sup>47</sup> Furthermore, as we have previously demonstrated,<sup>48</sup> 14,15-EET can activate EP<sub>4</sub>, raising the possibility that the effect observed in that study could also be mediated via 14,15-EET.

When we observed capillaries over time under basal conditions (no whisker stimulation), we discovered that approximately one third of capillaries undergo an increase in flux, one third show a decrease and one third show no change. This observation is consistent with capillary fluctuations and transit time heterogeneity. However, overall, since each of the three activities (increase/decrease/no change in flux) happens at an equal frequency, the net result is no change in overall flow in the capillary network in the resting state. During neuronal activation, the percentage of capillaries exhibiting a rise in flux increases at the expense of capillaries showing a drop in flux, with no difference in the percentage of capillaries undergoing no change. This suggests that capillaries respond to neuronal activation by redistributing blood flow, likely shifting blood flow to capillaries adjacent to active neurons. Since the proportion of capillaries with enhanced flux increases, while those with reduced flux decreases, there is a net effect in the capillary bed of increased flow. This concept has been validated by a recent study.<sup>49</sup> Using mouse retinal preparation, authors show that pericytes residing at capillary junctions differentially constrict to regulate capillary branch-specific blood flow, and that pericytes receiving propagating retrograde hyperpolarization channel RBCs toward active neurons. We should note here that although most capillaries within a network show increased flux, some do not respond to neuronal activation, and

others even exhibit reduced flux. This network-level response may help resolve some controversies regarding capillary involvement in the generation of functional hyperemia. For example, capillaries that showed constriction in response to whisker stimulation have been regarded as “random changes and measurement error.”<sup>1</sup> Furthermore, studies that reported no change in capillary diameter during functional hyperemia<sup>10</sup> may have looked at single capillaries in isolation, rather than as part of a network.

In further characterizing the capillary response in functional hyperemia, we make an intriguing observation that capillary diameter undergoes the same degree of change (10% change in diameter) during dilation and constriction. In other words, capillaries, seem to alternate between two distinct states (plus or minus 10% diameter). We speculate that this change is sufficient to either allow or block RBC passage through the capillary. Since RBCs are very close in size to inner capillary diameter, a slight decrease in diameter (the 10% that we see), may be sufficient to block RBC flux through a capillary. The broader implication is that unlike arterial and arteriolar blood flow, which is regulated by changes over a continuum of vessel tone,<sup>7</sup> capillary flow is regulated by switching “ON” some capillaries, and turning others “OFF”; thus redistributing RBCs within the network to ensure sufficient perfusion pressure and blood flow to where it is needed. Gonzales et al. determined the magnitude of the change in retinal capillary diameter in response to thromboxane A2 receptor agonist U46619, the depolarizing effect of 60 mM K<sup>+</sup>, and the relaxing effect of calcium-free solution.<sup>49</sup> Interestingly, they found varying responses in different branching order capillaries. Specifically, they found that first to third order capillaries constricted by ~35% in response to U46619 and by ~15% in response to 60 mM K<sup>+</sup>, and dilated by 5% to in calcium-free solution. On the other hand, fourth order capillaries and beyond responded U46619 only by 5%, but did not respond to 60 mM KCl or Ca<sup>2+</sup>-free solution. In our study, we find the change in diameter around 10% for both dilation and constriction regardless of the agent used. The discrepancy between our study and the study by Gonzales et al. could be related to their use of an isolated retinal preparation compared to our in vivo cerebrocortical imaging. For example, constriction could be exaggerated when capillaries are devoid of intraluminal fluids. Furthermore, the differences in the magnitude of constriction or dilation in different capillary segments in the study by Gonzalez et al. were attributed to different pericyte coverage densities in different segments. Therefore, differences in pericyte density between the retina and cerebral cortex may account for different results. Finally, it is possible that our analysis averaged

changes across different capillary segments. However, our analysis also focused on first to third branching order capillaries. Nonetheless, differences in vascular architecture between retina and cortex makes it difficult to perfectly match capillary segments between cortex and retina.

Due to the technical limitations of intravital imaging in mice, the results of our study should be interpreted with caution. Specifically, we used two different approaches to evaluate the vascular response to whisker stimulation: OCT-based flux and diameter changes in capillaries and two-photon microscopy (2PM)-based velocity measurement in arterioles. The more straightforward and direct approach to compare vascular responses to neuronal activation would have been to measure vascular diameter changes (dilation). It should be noted, however, that capillaries and arterioles are regulated by multiple mechanisms, some of which are specific to each segment, while others are shared by both segments. For example, we have previously reported that astrocyte-derived EETs mediate arteriolar dilation to neuronal activity.<sup>12–14</sup> In such a scenario, arteriolar dilation is directly linked to the activity of adjacent neurons and is the first vascular parameter to respond (see Figure 5). If, on the other hand, the two vessel segments are linked by a shared mechanism, as in retrograde vasodilation,<sup>40,50</sup> whereby capillary dilation drives upstream arteriolar dilation, then the change in arteriolar diameter could be secondary to an increase in arteriolar velocity as a result of decreased downstream resistance and increased shear stress (shear- or flow-mediated dilation). Others have been able to calculate RBC flow based on diameter and velocity, measured simultaneously using both longitudinal and cross-sectional scans.<sup>51</sup> The advantage of OCT is its deeper penetration and wider coverage of brain tissue volume, whereas 2PM has the advantage of higher resolution, but it is limited by a small and superficial imaging area (<200 μm vs. up 500 μm for OMAG). However, comparing flux to velocity in different size vessels may not be valid, since RBC velocity can remain unchanged yet RBC flow (volumetric flow) can increase if the vessel becomes dilated. Furthermore, fluid and cell components of the blood move at different rates and are likely affected differently by vessel contraction. As can be seen in Supplemental Figure 2, when we overlaid capillary flux with inverse mean intensity for arterioles (an approximation of volumetric flow), the peak of the inverse mean intensity of the arterioles has an even longer time delay than the peak of the velocity. One interpretation of this difference is that fluid picks up speed first, followed by a subsequent increase in RBC flow. Finally, it is possible that our results were impacted by tissue inflammation caused by the cranial window surgery. This concern can be

alleviated by conducting measurements through a chronically implanted window, at least two weeks after surgery, or by using a thinned-skull cranial window, rather than an open cranial window. Studies in rats and mice have shown using GFAP and Iba-1 immunoreactivity that inflammation under a cranial window resolves by two to four weeks after surgery.<sup>52,53</sup>

In summary, we provide evidence supporting the idea that cortical capillaries are involved in functional hyperemia, and that capillary response precedes that of arterioles. We further characterize the physiological response of capillaries, demonstrating that capillaries respond in a coordinated network-level manner. Lastly, we establish the role of endothelial 14,15-EET in pericyte-mediated maintenance of capillary basal tone and response to neuronal activation.

### Funding

The author(s) disclosed receipt of the following financial support for the research, authorship, and/or publication of this article: American Heart Association Grant-In-Aid (16GRNT31380022) and NIH R01 (NS108501-01) to NJA.


### Declaration of conflicting interests



The author(s) declared no potential conflicts of interest with respect to the research, authorship, and/or publication of this article.

### Authors' contributions

WZ, DMZ, KG executed experiments and analyzed data. CMD organized and interpreted data, drafted the manuscript. MXW, MH, DH, YL analyzed data. RKW developed imaging and analysis method. JJI designed 2PM studies. NJA conceived the project, designed studies, interpreted data and drafted manuscript. All authors revised and approved the final submission.

### ORCID iDs

Catherine M Davis  <https://orcid.org/0000-0001-9654-3509>  
Douglas M Zeppenfeld  <https://orcid.org/0000-0002-1800-649X>

Marie X Wang  <https://orcid.org/0000-0002-2492-7332>  
Nabil J Alkayed  <https://orcid.org/0000-0002-3489-4730>

### Supplementary material

Supplemental material for this article is available online.

### References

1. Hall CN, Reynell C, Gesslein B, et al. Capillary pericytes regulate cerebral blood flow in health and disease. *Nature* 2014; 508: 55–60.
2. Rungta RL, Chaigneau E, Osmanski BF, et al. Vascular compartmentalization of functional hyperemia from the synapse to the pia. *Neuron* 2018; 99: 362–375.

3. Hamilton NB, Attwell D and Hall CN. Pericyte-mediated regulation of capillary diameter: a component of neurovascular coupling in health and disease. *Front Neuroenerget* 2010; 2: 5.
4. Nippert AR, Biesecker KR and Newman EA. Mechanisms mediating functional hyperemia in the brain. *Neuroscientist* 2018; 24: 73–83.
5. Kornfield TE and Newman EA. Regulation of blood flow in the retinal trilaminar vascular network. *J Neurosci* 2014; 34: 11504–11513.
6. Peppiatt CM, Howarth C, Mobbs P, et al. Bidirectional control of CNS capillary diameter by pericytes. *Nature* 2006; 443: 700–704.
7. Tian P, Teng IC, May LD, et al. Cortical depth-specific microvascular dilation underlies laminar differences in blood oxygenation level-dependent functional MRI signal. *Proc Natl Acad Sci USA* 2010; 107: 15246–15251.
8. Winkler EA, Sagare AP and Zlokovic BV. The pericyte: a forgotten cell type with important implications for Alzheimer's disease? *Brain Pathol* 2014; 24: 371–386.
9. Alarcon-Martinez L, Yilmaz-Ozcan S, Yemisci M, et al. Capillary pericytes express  $\alpha$ -smooth muscle actin, which requires prevention of filamentous-actin depolymerization for detection. *Elife* 2018; 7: e34861.
10. Fernández-Klett F, Offenhauser N, Dirnagl U, et al. Pericytes in capillaries are contractile in vivo, but arterioles mediate functional hyperemia in the mouse brain. *Proc Natl Acad Sci USA* 2010; 107: 22290–22295.
11. Hill RA, Tong L, Yuan P, et al. Regional blood flow in the normal and ischemic brain is controlled by arteriolar smooth muscle cell contractility and not by capillary pericytes. *Neuron* 2015; 87: 95–110.
12. Alkayed NJ, Birks EK, Narayanan J, et al. Role of P-450 arachidonic acid epoxygenase in the response of cerebral blood flow to glutamate in rats. *Stroke* 1997; 28: 1066–1072.
13. Harder DR, Alkayed NJ, Lange AR, et al. Functional hyperemia in the brain: hypothesis for astrocyte-derived vasodilator metabolites. *Stroke* 1998; 29: 229–234.
14. Peng X, Carhuapoma JR, Bhardwaj A, et al. Suppression of cortical functional hyperemia to vibrissal stimulation in the rat by epoxygenase inhibitors. *Am J Physiol Heart Circ Physiol* 2002; 283: H2029–H2037.
15. Peng X, Zhang C, Alkayed NJ, et al. Dependency of cortical functional hyperemia to forepaw stimulation on epoxygenase and nitric oxide synthase activities in rats. *J Cereb Blood Flow Metab* 2004; 24: 509–517.
16. Baran U, Zhu W, Choi WJ, et al. Automated segmentation and enhancement of optical coherence tomography-acquired images of rodent brain. *J Neurosci Methods* 2016; 270: 132–137.
17. Methner C, Mishra A, Golgotiu K, et al. Pericyte constriction underlies capillary derecruitment during hyperemia in the setting of arterial stenosis. *Am J Physiol Heart Circ Physiol* 2019; 317: H255–H263.
18. Du Sert NP, Hurst V, Ahluwalia A, et al. The ARRIVE guidelines 2.0: updated guidelines for reporting animal research. *J Cereb Blood Flow Metab* 2020; 40: 1769–1777.
19. Zhang W, Davis CM, Edin ML, et al. Role of endothelial soluble epoxide hydrolase in cerebrovascular function and ischemic injury. *PLoS One* 2013; 8: e61244.
20. Iliff JJ, Fairbanks SL, Balkowiec A, et al. Epoxyeicosatrienoic acids are endogenous regulators of vasoactive neuropeptide release from trigeminal ganglion neurons. *J Neurochem* 2010; 115: 1530–1542.
21. Gauthier KM, Jagadeesh SG, Falck JR, et al. 14,15-epoxyeicosa-5(Z)-enoic-mSI: a 14,15- and 5,6-EET antagonist in bovine coronary arteries. *Hypertension* 2003; 42: 555–561.
22. Cai C, Fordsmann JC, Jensen SH, et al. Stimulation-induced increases in cerebral blood flow and local capillary vasoconstriction depend on conducted vascular responses. *Proc Natl Acad Sci USA* 2018; 115: E5796–E5804.
23. Wang RK, Jacques SL, Ma Z, et al. Three dimensional optical angiography. *Opt Express* 2007; 15: 4083–4097.
24. Chen CL and Wang RK. Optical coherence tomography based angiography. *Biomed Opt Express* 2017; 8: 1056–1082.
25. Wang RK. Optical microangiography: a label-free 3-D imaging technology to visualize and quantify blood circulations within tissue beds in vivo. *IEEE J Sel Top Quantum Electron* 2010; 16: 545–554.
26. Chu Z, Lin J, Gao C, et al. Quantitative assessment of the retinal microvasculature using optical coherence tomography angiography. *J Biomed Opt* 2016; 21: 66008.
27. Alkayed NJ, Narayanan J, Gebremedhin D, et al. Molecular characterization of an arachidonic acid epoxygenase in rat brain astrocytes. *Stroke* 1996; 27: 971–979.
28. Davis CM, Siler DA and Alkayed NJ. Endothelium-derived hyperpolarizing factor in the brain: influence of sex, vessel size and disease state. *Womens Health (Lond)* 2011; 7: 293–303.
29. Gauthier KM, Deeter C, Krishna UM, et al. 14,15-Epoxyeicosa-5(Z)-enoic acid: a selective epoxyeicosatrienoic acid antagonist that inhibits endothelium-dependent hyperpolarization and relaxation in coronary arteries. *Circ Res* 2002; 90: 1028–1036.
30. Hillman EM. Coupling mechanism and significance of the BOLD signal: a status report. *Annu Rev Neurosci* 2014; 37: 161–181.
31. Kuschinsky W and Paulson OB. Capillary circulation in the brain. *Cerebrovasc Brain Metab Rev* 1992; 4: 261–286.
32. Jespersen SN and Østergaard L. The role of cerebral blood flow, capillary transit time heterogeneity, and oxygen tension in brain oxygenation and metabolism. *J Cereb Blood Flow Metab* 2012; 32: 264–277.
33. Stefanovic B, Hutchinson E, Yakovleva V, et al. Functional reactivity of cerebral capillaries. *J Cereb Blood Flow Metab* 2008; 28: 961–972.
34. Larsson HBW, Vestergaard MB, Lindberg U, et al. Brain capillary transit time heterogeneity in healthy volunteers measured by dynamic contrast-enhanced T1-weighted perfusion MRI. *J Magn Reson Imag* 2017; 45: 1809–1820.
35. Chuang KH, van Gelderen P, Merkle H, et al. Mapping resting-state functional connectivity using perfusion MRI. *Neuroimage* 2008; 40: 1595–1605.

36. Rogers BP, Morgan VL, Newton AT, et al. Assessing functional connectivity in the human brain by fMRI. *Magn Reson Imag* 2007; 25: 1347–1357.
37. Martuzzi R, Ramani R, Qiu M, et al. Functional connectivity and alterations in baseline brain state in humans. *Neuroimage* 2010; 49: 823–834.
38. Wei HS, Kang H, Rasheed ID, et al. Erythrocytes are oxygen-sensing regulators of the cerebral microcirculation. *Neuron* 2016; 91: 851–862.
39. Kisler K, Nelson AR, Rege SV, et al. Pericyte degeneration leads to neurovascular uncoupling and limits oxygen supply to brain. *Nat Neurosci* 2017; 20: 406–416.
40. Longden TA, Dabertrand F, Koide M, et al. Capillary K<sup>+</sup>-sensing initiates retrograde hyperpolarization to increase local cerebral blood flow. *Nat Neurosci* 2017; 20: 717–726.
41. Gupta NC, Davis CM, Nelson JW, et al. Soluble epoxide hydrolase: sex differences and role in endothelial cell survival. *Arterioscler Thromb Vasc Biol* 2012; 32: 1936–1942.
42. Carver KA, Lourim D, Tryba AK, et al. Rhythmic expression of cytochrome P450 epoxygenases CYP4x1 and CYP2c11 in the rat brain and vasculature. *Am J Physiol Cell Physiol* 2014; 307: C989–98.
43. Zhao Z, Nelson AR, Betsholtz C, et al. Establishment and dysfunction of the blood-brain barrier. *Cell* 2015; 163: 1064–1078.
44. Davis CM, Liu X and Alkayed NJ. Cytochrome P450 eicosanoids in cerebrovascular function and disease. *Pharmacol Ther* 2017; 179: 31–46.
45. Chen BR, Kozberg MG, Bouchard MB, et al. A critical role for the vascular endothelium in functional neurovascular coupling in the brain. *J Am Heart Assoc* 2014; 3: e000787.
46. Mishra A, Reynolds JP, Chen Y, et al. Astrocytes mediate neurovascular signaling to capillary pericytes but not to arterioles. *Nat Neurosci* 2016; 19: 1619–1627.
47. Spector AA and Kim HY. Cytochrome P450 epoxygenase pathway of polyunsaturated fatty acid metabolism. *Biochim Biophys Acta* 2015; 1851: 356–365.
48. Liu X, Qian ZY, Xie F, et al. Functional screening for G protein-coupled receptor targets of 14,15-epoxyeicosatrienoic acid. *Prostaglandins Other Lipid Mediat* 2017; 132: 31–40.
49. Gonzales AL, Klug NR, Moshkforoush A, et al. Contractile pericytes determine the direction of blood flow at capillary junctions. *Proc Natl Acad Sci USA* 2020; 117: 27022–27033.
50. Iadecola C, Yang G, Ebner T, et al. Local and propagated vascular responses evoked by focal synaptic activity in cerebellar cortex. *J Neurophysiol* 1997; 78: 651–659.
51. Shih AY, Driscoll JD, Drew PJ, et al. Two-photon microscopy as a tool to study blood flow and neurovascular coupling in the rodent brain. *J Cereb Blood Flow Metab* 2012; 32: 1277–1309.
52. Holtmaat A, Bonhoeffer T, Chow DK, et al. Long-term, high-resolution imaging in the mouse neocortex through a chronic cranial window. *Nat Protoc* 2009; 4: 1128–1144.
53. Koletar MM, Dorr A, Brown ME, et al. Refinement of a chronic cranial window implant in the rat for longitudinal in vivo two-photon fluorescence microscopy of neurovascular function. *Sci Rep* 2019; 9: 5499.